Yao LIU
Yashun WANG
Zhengwei FAN
Zhanqiang HOU
Shufeng ZHANG
Xun CHEN

LIFETIME PREDICTION METHOD FOR MEMS GYROSCOPE BASED ON ACCELERATED DEGRADATION TEST AND ACCELERATION FACTOR MODEL

METODA PROGNOZOWANIA CZASU PRACY ŻYROSKOPU MEMS NA PODSTAWIE TESTU PRZYSPIESZONEJ DEGRADACJI I MODELU WSPÓŁCZYNNIKA PRZYSPIESZENIA

The reliability analysis of MEMS gyroscope under long-term operating condition has become an urgent requirement with the enlargement of its application scope and the requirement of good durability. In this study we propose a lifetime prediction method for MEMS gyroscope based on accelerated degradation tests (ADTs) and acceleration factor model. Firstly, the degradation characteristic (bias instability) is extracted based on Allan variance. The effect of temperature stress on the degradation rate of bias instability is analyzed, and it shows that the degradation rate of bias instability would increase with the increase of the temperature. Secondly, the ADTs of MEMS gyroscope are designed and conducted, the degradation model of MEMS gyroscope is established based on the output voltage of MEMS gyroscope and Allan variance. Finally, the acceleration factor model of MEMS gyroscope under temperature stress is derived, and the lifetime of the MEMS gyroscope is predicted based on two group tests data under high stress level. The results show that the lifetime calculated by the acceleration factor model and mean lifetime under high stress levels is close to the mean lifetime calculated by the linear equation at normal temperature stress.

Keywords: *MEMS gyroscope, temperature stress, accelerated degradation test, acceleration factor model, Allan variance.*

Analiza niezawodności żyroskopu MEMS w warunkach długotrwałej pracy stała się pilną koniecznością wraz z rozszerzeniem zakresu jego zastosowania i wprowadzeniem wymogu dobrej trwałości. W niniejszym artykule, zaproponowano metodę prognozowania czasu pracy żyroskopu MEMS w oparciu o testy przyspieszonej degradacji i model współczynnika przyspieszenia. W pierwszej kolejności, wyznaczono charakterystykę degradacji (niestabilność wskazań) na podstawie wariancji Allana. Analizowano wpływ naprężenia cieplnego na szybkość degradacji w zakresie niestabilności wskazań. Analiza wykazała, że szybkość degradacji wzrastała wraz ze wzrostem temperatury. Następnie, opracowano i przeprowadzono testy przyspieszonej degradacji żyroskopu MEMS, a model jego degradacji ustalono na podstawie napięcia wyjściowego żyroskopu i wariancji Allana. Na koniec, wyprowadzono model współczynnika przyspieszenia dla żyroskopu MEMS w warunkach naprężenia cieplnego, a żywotność żyroskopu prognozowano na podstawie danych z dwóch testów grupowych przeprowadzonych w warunkach wysokiego naprężenia. Wyniki pokazują, że czas pracy obliczony na podstawie modelu współczynnika przyspieszenia i średni czas pracy przy wysokich poziomach naprężeń są zbliżone do średniego czasu pracy obliczonego na podstawie równania liniowego przy normalnym naprężeniu cieplnym.

Słowa kluczowe: *żyroskop MEMS, naprężenie cieplne, test przyspieszonej degradacji, model współczynnika przyspieszenia, wariancja Allana.*

1. Introduction

MEMS gyroscopes, due to its lower mass, lower power consumption, and smaller volume, have become one of the most promising inertial components, widely used in commercial, military and other fields [13], such as inertial navigation devices, portable electronic products and so on. However, MEMS gyroscopes often undergo high temperature condition, and physical properties of silicon materials would be significantly affected by temperature. How to predict the lifetime of the MEMS gyroscope has become an urgent problem to be solved in engineering [32].

Accelerated degradation test (ADT) collects performance degradation data of products at accelerated stress levels, and uses these data to extrapolate reliability and lifetime of products for the use conditions [20, 23, 33, 34]. Mulloni studied the lifetime prediction of RF-MEMS switches based on ADT [22]. The reliable lifetime of the smart electricity meter was predicted by an accelerated degradation test and degradation model [17, 35]. Wang [33] made a research on the lifetime prediction of self-lubricating spherical plain bearings based on the ADT. An ADT of light bars was tested under different stresses, and a response model based on an inverse power (exponential) law for the failure time under different stresses was then calculated to predict the

lifetime under operating conditions [10]. A progressive-stress acceler-ated degradation test with a non-linear degradation path was proposed to obtain timely information of the product's lifetime distribution for highly reliable products [6]. Chen studied the accelerated degradation reliability modeling and test data statistical analysis of aerospace electrical connector [5]. Lifetime prediction technology based on ADT has become an inevitable requirement for reliability prediction of MEMS gyroscopes under time and cost constraints [4, 31].

The selection of accelerated stress is the first step in the imple-mentation of ADT. Many scholars have studied the effect of tempera-ture on the performance of MEMS device. Jin-Won Joo studied the global and local deformations of packages caused by temperature, and studied the influence of temperature on frequency shift of MEMS gy-roscope [15]. Chun-Lin Lu analyzed the thermal stress for a CMOS-MEMS microphone with various metallization and materials [8]. Saeedivahdat et al. studied the effect of thermal stress on frequency response for a diaphragm in MEMS microphone by numerical model [29]. Therefore, temperature stress may be the most likely accelerated stress of MEMS gyroscope in ADTs.

Extraction of degradation characteristic is the key step to establish degradation model [25, 30]. There are many noise terms in the output voltage of MEMS gyroscope due to its working principle and process-ing technology, which makes the extraction of the effective degrada-tion characteristics more complicated. Many scholars have studied the noise terms by power spectral density (PSD), time domain analysis methods (autocorrelation function, Gauss Markov process and autore-gressive model) and the Kalman filter method. However, these meth-ods have their own inherent shortcomings [16, 19, 36].

Allan variance is an important means to analyze the random noise characteristics of gyroscope, including laser gyroscope, fiber optic gyroscope and MEMS gyroscope. The method is a time domain analysis method proposed by the American National Bureau of Standards, which has been an IEEE standard method for parameter analysis of gyroscopes [9]. Allan variance usually describe the noise of gyroscope as several stochastic character-istics: quantization noise, angular random walk, bias instability, rate random walk and rate ramp. Some stochastic characteris-tics often directly reflect the performance of gyroscope, such as angular random walk and bias instability [1-3].

Many scholars have studied the performance of laser gyro-scope and fiber optic gyroscope based on Allan variance. Law-rence analyzed the performance of ring laser gyroscope based on Allan variance [18]. Pin analyzed the noise characteristics of fiber optic gyroscope based on weighted least squares al-gorithm and Allan variance [26]. Grantham ana-lyzed the random error of inertial sensors us-ing Allan variance [11]. Chikovani evaluated the performance of laser gyroscopes, and fiber optic gyroscopes from different countries based on Allan variance [7]. However, the research on performance study of MEMS gyroscope is limited.

The rest of this document is organized as follows. In Section 2, we extract the degrada-tion characteristic (bias instability) of MEMS gyroscope based on Allan variance, and ana-lyze the effect of temperature stress on the deg-radation rate of bias instability. In Section 3, a universal lifetime prediction method of MEMS gyroscope is proposed. In Section 4, a case study is provided to illustrate the application and utility of the proposed method. Finally, the conclusions are presented in Section 5.

2. Theory

2.1. Structure and operating principle of MEMS gyroscope

Almost all MEMS gyroscope use vibrating mechanical elements to sense rotation, ''Butterfly'' MEMS gyroscope is a typical vibrating MEMS gyroscope based on the Coriolis effect [14]. As shown in Fig-ure1, it has a four-mass full-differential structure with high sensitivity, good linearity and low cost, and is widely used in commercial fields.

"Butterfly" MEMS gyroscope mainly contains the circuit board and the vacuum packaged resonator, as shown in Figure 1(a). The image of resonator is shown in Figure 1(b), which consists of a single crystal silicon structure and a Pyrex glass base with patterned elec-trodes [14]. The silicon structure is manufactured by anisotropic wet etching process, which mainly includes four proof masses, a slanted suspension beam, and four trapezoidal cantilever beams, as shown in Figure 2(a). The excitation electrodes and detection electrodes are fabricated on Pyrex glass base under the proof mass, as shown in Fig-ure 2(b), and it is connected with silicon structure by anodic bonding to form driving capacitance and detecting capacitance. The cross sec-tion of the slanted suspension beam (A-A) is composed of (100) and (111) crystal planes with an angle of 54.74°, as shown in Figure 2(c).

The slanted beam with an asymmetric cross section so that vertical electrostatic forces bend the beams both vertically and horizontally, as shown in Figure 2(c). The excitation mode is the flexural vibration of the slanted beam; the detection mode is the torsional vibration of the slanted beam. The excitation mode and the detection mode are two perpendicular degenerate modes of the axially symmetric elastic body. There will be a sinusoidal oscillation in detection axis direction due to the Coriolis Effect when an angular rate inputs.
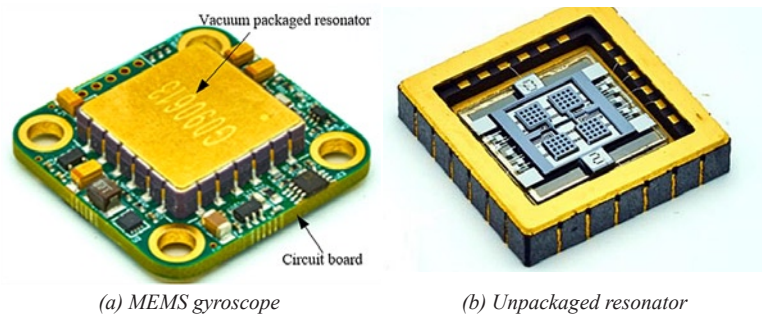

(a) MEMS gyroscope   *(b) Unpackaged resonator*

Fig. 1. *EG136A type MEMS gyroscope , which consists of the circuit board and the vacu-um packaged resonator*
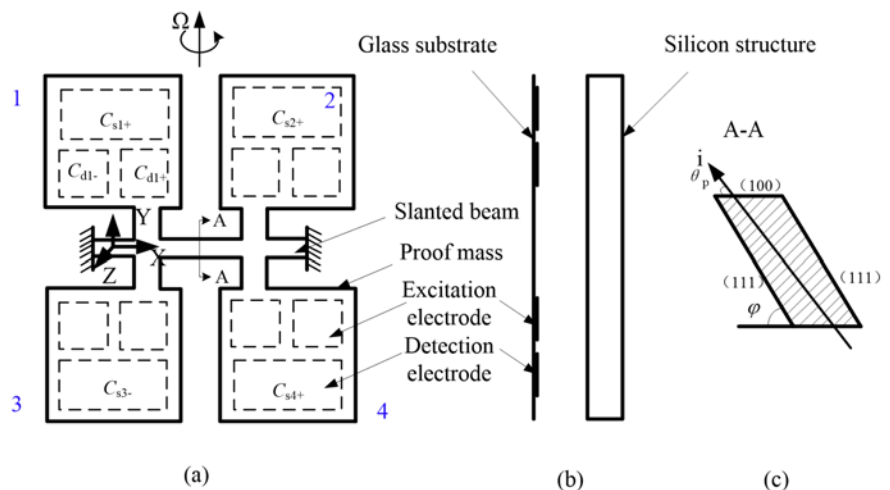

Fig. 2 Silicon structure and the electrode layout of ''Butterfly'' MEMS gyroscope

Electrostatic force from the excitation electrodes makes the four proof masses vibrate with stable amplitude and phase on its resonant frequency by automatic gain control methods. There will be an oscillation in detection axis (Z direction) due to the Coriolis Effect if there is an angular rate in the sensitive axis (Y direction), which reflects the value of the input angular rate.

2.2. The principle of Allan variance

Allan Variance is a method of describing the root mean square of random drift error. Sampling the angular rate of MEMS gyroscope with sampling time τ_0, and the total sample size is M. Then m ($m=\tau_0$, $2\tau_0$, ..., $M/2\tau_0$]) data points are made as one cluster, so we can get $J=[M/m]$ clusters, where $[x]$ represents the floor of x. J is the number of sampled groups. The time of each group $\tau=m\tau_0$ is the correlation time, and the average value of the defined angular rate can be expressed as:

$$\bar{w}_k(m) = \frac{1}{m}\sum_{i=1}^{m} w_{(k-1)m+i} \qquad k=1,2,\cdots\left[\frac{M}{2}\right] \qquad (1)$$

The Allan variance defined by the angular rate can be expressed as:

$$\sigma^2(\tau) = \frac{1}{2(J-1)}\sum_{k=1}^{J-1}\left[\bar{w}_{k+1}(m) - \bar{w}_k(m)\right]^2 \qquad (2)$$

where $\langle y \rangle$ represents the average of y.

Allan variance can usually subdivide the random noise characteristics of the inertial device (MEMS gyroscope) into five typical characteristics, namely quantization noise, angular random walk, bias instability, and rate random walk and rate ramp. It can be expressed as [28]:

$$\begin{cases} \sigma_Q^2 = 3Q^2/\tau^2 \\ \sigma_N^2 = N^2/\tau \\ \sigma_B^2 = 2\ln 2/\pi\, B_s^2 \\ \sigma_K^2 = \kappa^2\tau/3 \\ \sigma_R^2 = R^2\tau^2/2 \end{cases} \qquad (3)$$

where Q is a random drift caused by quantization noise. The initial output of the inertial sensor is analog data, which is quantized into digital data for calculation, thus quantization noise is generated at the output of the inertia device [26]. N is the white noise generated during the measurement process, which appears as an angular random walk at the output of the MEMS gyro and belongs to high frequency noise [19]. B_s is a random drift caused by bias instability, which is a kind of low-frequency noise generated by the sensor electronic components or the surrounding environment [26]. κ is a random drift caused by random walk. The source of this error is still unclear. R is the random drift caused by the rate ramp, which is caused by the monotonic change of the sensor for a long time [26].

It is generally considered that five typical characteristics are independent of each other, so the total variance can be expressed as [24]:

$$Y = X\beta + e \qquad (4)$$

where:

$$Y = \begin{bmatrix} \sigma_1^2 \\ \sigma_2^2 \\ \vdots \\ \sigma_m^2 \end{bmatrix}, \quad X = \begin{bmatrix} \tau_1^{-2} & \tau_1^{-1} & 1 & \tau_1^1 & \tau_1^2 \\ \tau_2^{-2} & \tau_2^{-1} & 1 & \tau_2^1 & \tau_2^2 \\ \vdots & \vdots & \vdots & \vdots & \vdots \\ \tau_m^{-2} & \tau_m^{-1} & 1 & \tau_m^1 & \tau_m^2 \end{bmatrix}, \quad \beta = \begin{bmatrix} 3Q^2 \\ N^2 \\ (2\ln 2/\pi\, B_s)^2 \\ \kappa^2/3 \\ R^2/2 \end{bmatrix} \text{ and, } e = \begin{bmatrix} w_1 \\ w_2 \\ \vdots \\ w_m \end{bmatrix} \qquad (5)$$

Five unknown parameters Q, N, B_s, κ, R can be obtained by the least squares algorithm:

$$\beta = \left(X^T X\right)^{-1} X^T Y \qquad (6)$$

2.3. The effect of temperature stress on the degradation rate of bias instability

Bias instability of MEMS gyroscope in a certain period of time can be calculated by Allan variance. In order to characterize the degradation characteristic changing with time, we calculate the bias instability using daily data, so the bias instability in D days are B_s^1, B_s^2 ..., B_s^D respectively.

The five characteristics of the MEMS gyroscope under long-term operation (D days) can be expressed as:

$$\beta_t = \left(X^T X\right)^{-1} X^T Y_t \qquad (t=1,2,3,...,D) \qquad (7)$$

where:

$$Y_t = \begin{bmatrix} \sigma_{t1}^2 \\ \sigma_{t2}^2 \\ \vdots \\ \sigma_{tm}^2 \end{bmatrix}, \quad X = \begin{bmatrix} \tau_1^{-2} & \tau_1^{-1} & 1 & \tau_1^1 & \tau_1^2 \\ \tau_2^{-2} & \tau_2^{-1} & 1 & \tau_2^1 & \tau_2^2 \\ \vdots & \vdots & \vdots & \vdots & \vdots \\ \tau_m^{-2} & \tau_m^{-1} & 1 & \tau_m^1 & \tau_m^2 \end{bmatrix} \text{ and, } \beta_t = \begin{bmatrix} 3Q_t^2 \\ N_t^2 \\ (2\ln 2/\pi\, B_s^t)^2 \\ \kappa_t^2/3 \\ R_t^2/2 \end{bmatrix} \qquad (8)$$

where σ_{tm}^2 is the calculated Allan variance of the t-th day. Q_t is the quantization noise of the t-th day, N_t is the angular random walk of the t-th day, B_s^t is the bias instability of the t-th day, κ_t is the rate ramp of the t-th day, and R_t is the rate random walk of the t-th day.

Equation (7) can also be simplified as:

$$\beta_t = A_{5\times m} Y_t \qquad (t=1,2,3,...,D) \qquad (9)$$

In order to study the bias instability B_s in the vector β_t, it assumed that the elements of the third row in the matrix A are $a_{31}, a_{32}, a_{33}... a_{3m}$, so equation (9) can be further simplified as:

$$\left(2\ln 2/\pi\, B_s(t)\right)^2 = \left[a_{3,1}, a_{3,2}, a_{3,3}, a_{3,m}\right]\begin{bmatrix} \sigma_{t,1}^2 \\ \sigma_{t,2}^2 \\ \vdots \\ \sigma_{t,m}^2 \end{bmatrix} = a_{3,1}\sigma_{t,1}^2 + a_{3,2}\sigma_{t,2}^2 + \cdots + a_{3,m}\sigma_{t,m}^2 \qquad (10)$$

The bias instability change with time can be expressed as (equation (11) is verified in Section 4.3):

$$B_s^t = B_s(t) = Kt + b \qquad (11)$$

where K is degradation rate of the bias instability, and b is the intercept.

Substituting equation (11) into equation (10), equation (10) can also be expressed as:

$$\left[0.6643 B_s(t) \right]^2 = \left[0.6643(Kt+b) \right]^2 = a_{3,1}\sigma_{t,1}^2 + a_{3,2}\sigma_{t,2}^2 + \cdots + a_{3,m}\sigma_{t,m}^2 \qquad (12)$$

Partial derivatives for temperature in both sides of equation (12), we can get:

$$0.8826(Kt+b)\frac{\partial K}{\partial T} = \frac{\partial \left(a_{3,1}\sigma_{t,1}^2 + a_{3,2}\sigma_{t,2}^2 + \cdots + a_{3,m}\sigma_{t,m}^2 \right)}{\partial T} \qquad (13)$$

Equations (7)-(9) show that the third row elements $a_{31}, a_{32}, a_{33}... a_{3m}$ in matrix A are only related to the correlation time τ, so the right term of the equation (13) can be written as:

$$\frac{\partial \left(a_{3,1}\sigma_{t,1}^2 + a_{3,2}\sigma_{t,2}^2 + \cdots + a_{3,m}\sigma_{t,m}^2 \right)}{\partial T} = a_{3,1}\frac{\partial \sigma_{t,1}^2}{\partial T} + a_{3,2}\frac{\partial \sigma_{t,2}^2}{\partial T} + a_{3,3}\frac{\partial \sigma_{t,3}^2}{\partial T} + \cdots + a_{3,m}\frac{\partial \sigma_{t,m}^2}{\partial T} \qquad (14)$$

Substituting equation (2) into equation (14), equation (14) can be expressed as:

$$a_{3,1}\frac{\partial \sigma_{t,1}^2}{\partial T} + a_{3,2}\frac{\partial \sigma_{t,2}^2}{\partial T} + a_{3,3}\frac{\partial \sigma_{t,3}^2}{\partial T} + \cdots + a_{3,m}\frac{\partial \sigma_{t,m}^2}{\partial T}$$

$$= \frac{a_{3,1}}{2(J-1)}\sum_{k=1}^{J-1}\frac{\partial \left[\bar{w}_{k+1}(1) - \bar{w}_k(1) \right]^2}{\partial T} + \frac{a_{3,2}}{2(J-1)}\sum_{k=1}^{J-1}\frac{\partial \left[\bar{w}_{k+1}(2) - \bar{w}_k(2) \right]^2}{\partial T}$$

$$+ \frac{a_{3,m}}{2(J-1)}\sum_{k=1}^{J-1}\frac{\partial \left[\bar{w}_{k+1}(m) - \bar{w}_k(m) \right]^2}{\partial T} \qquad (15)$$

The first term in equation (15) denotes the square of the difference between adjacent arrays when the correlation time $\tau=1$. Substituting equation (1) into the first item of equation (15), we can get:

$$\frac{a_{3,1}}{2(J-1)}\sum_{k=1}^{J-1}\frac{\partial \left[\bar{w}_{k+1}(1) - \bar{w}_k(1) \right]^2}{\partial T}$$

$$= \frac{a_{3,1}}{2(J-1)}\sum_{k=1}^{J-1}\frac{\partial \left[w_{k+1} - w_k \right]^2}{\partial T} \qquad (16)$$

It is assumed that all the parameters (electrical parameters and structural parameters) of the MEMS gyroscope do not change during the operating process, only the environment temperature changes from T to $T+\Delta T$, resulting in the MEMS gyroscope's output (angular rate) changing from w_k to w_{k+1}, so equation (16) can be expressed as:

$$\frac{a_{3,1}}{2(J-1)}\sum_{k=1}^{J-1}\frac{\partial \left[\bar{w}_{k+1}(1) - \bar{w}_k(1) \right]^2}{\partial T}$$

$$= \frac{a_{3,1}}{2(J-1)}\sum_{k=1}^{J-1}\frac{\partial \left[w_{k+1}(T+\Delta T) - w_k(T) \right]^2}{\partial T} \qquad (17)$$

The second term in equation (15) denotes the square of the difference between adjacent arrays when the correlation time $\tau=2$. Substituting equation (1) into the first item of equation (15), we can get:

$$\frac{a_{3,2}}{2(J-1)}\sum_{k=1}^{J-1}\frac{\partial \left[\bar{w}_{k+1}(2) - \bar{w}_k(2) \right]^2}{\partial T}$$

$$= \frac{a_{3,2}}{2(J-1)}\sum_{k=1}^{J-1}\frac{\partial \left[\frac{1}{2}\sum_{i=1}^{2}w_{2k+i} - \frac{1}{2}\sum_{i=1}^{2}w_{2(k-1)+i} \right]^2}{\partial T} \qquad (18)$$

Similarly, it is assumed that all the parameters (electrical parameters and structural parameters) of the MEMS gyroscope do not change during the working process, only the environment temperature changes from T to $T+\Delta T$, resulting in the MEMS gyroscope's output (angular rate) changing from w_{2k+i} to $w_{2(k-1)+i}$, so equation (18) can be expressed as:

$$\frac{a_{3,2}}{2(J-1)}\sum_{k=1}^{J-1}\frac{\partial \left[\bar{w}_{k+1}(2) - \bar{w}_k(2) \right]^2}{\partial T}$$

$$= \frac{a_{3,2}}{8(J-1)}\sum_{k=1}^{J-1}\frac{\partial \left[\sum_{i=1}^{2}w_{2k+i}(T+\Delta T) - \sum_{i=1}^{2}w_{2(k-1)+i}(T) \right]^2}{\partial T} \qquad (19)$$

So the m-th term in equation (18) can be expressed as:

$$\frac{a_{3,m}}{2(J-1)}\sum_{k=1}^{J-1}\frac{\partial \left[\bar{w}_{k+1}(m) - \bar{w}_k(m) \right]^2}{\partial T}$$

$$= \frac{a_{3,m}}{2m^2(J-1)}\sum_{k=1}^{J-1}\frac{\partial \left[\sum_{i=1}^{m}w_{km+i}(T+\Delta T) - \sum_{i=1}^{m}w_{(k-1)m+i}(T) \right]^2}{\partial T} \qquad (20)$$

Substituting equation (17) equation (19) and equation (20) into equation (15), we can get:

$$a_{3,1}\frac{\partial \sigma_{t,1}^2}{\partial T} + a_{3,2}\frac{\partial \sigma_{t,2}^2}{\partial T} + a_{3,3}\frac{\partial \sigma_{t,3}^2}{\partial T} + \cdots + a_{3,m}\frac{\partial \sigma_{t,m}^2}{\partial T}$$

$$= \frac{a_{3,1}}{2(J-1)}\sum_{k=1}^{J-1}\frac{\partial \left[w_{k+1}(T+\Delta T) - w_k(T) \right]^2}{\partial T}$$

$$+ \frac{a_{3,2}}{2 \cdot 2^2(J-1)}\sum_{k=1}^{J-1}\frac{\partial \left[\sum_{i=1}^{2}w_{2k+i}(T+\Delta T) - \sum_{i=1}^{2}w_{2(k-1)+i}(T) \right]^2}{\partial T} \qquad (21)$$

$$+ ... + \frac{a_{3,m}}{2m^2(J-1)}\sum_{k=1}^{J-1}\frac{\partial \left[\sum_{i=1}^{m}w_{km+i}(T+\Delta T) - \sum_{i=1}^{m}w_{(k-1)m+i}(T) \right]^2}{\partial T}$$

It can be known that the solution of partial derivative is independent of the value of k from equation (21), without a loss of generality, let $k = 3$, we prove that the partial derivative is greater than 0. The proof process is as follows.

Let:

$$x(T + \Delta T) = \sum_{i=1}^{m} w_{3m+i}(T + \Delta T)$$

$$x(T) = \sum_{i=1}^{m} w_{2m+i}(T) \tag{22}$$

$\dfrac{\partial x(T)}{\partial T} > 0$ due to $\dfrac{\partial w}{\partial T} > 0$ [26], so:

$$\frac{\partial \left[x(T + \Delta T) - x(T) \right]^2}{\partial T} = 2\left[x(T + \Delta T) - x(T) \right] \frac{\partial x(T + \Delta T) - \partial x(T)}{\partial t} > 0 \tag{23}$$

So we can get:

$$\frac{\partial \left[\sum_{i=1}^{m} w_{3m+i}(T + \Delta T) - \sum_{i=1}^{m} w_{2m+i}(T) \right]^2}{\partial T} > 0 \tag{24}$$

Because the correlation time τ is positive, the third row elements of matrix A are all positive, so:

$$0.8826(Kt + b)\frac{\partial K}{\partial T} > 0 \tag{25}$$

Because the bias instability is larger than 0, so:

$$\frac{\partial K}{\partial T} > 0 \tag{26}$$

It indicates that the degradation rate of bias instability would increase with the increase of the temperature. So bias instability can be the degradation characteristic of MEMS gyroscope, and the temperature can be the accelerated stress of MEMS gyroscope in ADTs.

3. A universal lifetime prediction method of MEMS gyroscope

3.1. Model assumptions

The degradation of the product is affected by temperature stress. The degradation process of the product can be accelerated by the temperature stress higher than the use or storage conditions. In ADTs, the stress level of the accelerated stress is L. The setting of stress level of accelerated stress does not change the degradation mechanism of the product, that is, the degradation mechanism of the product in ADTs is consistent with that in normal use.

It is assumed that the theoretical degradation trajectory and accelerated degradation trajectory of the product satisfy the linear degradation model, which can be expressed as:

$$B_{s,ijk}(t|S_i) = K_i t + b_i + \varepsilon_{ijk}, \quad i = 1,2,...,M, j = 1,2,...,n_i, k = 1,2,...,l_i \tag{27}$$

where $B_{s,ijk}$ is the characteristic value (bias instability) of the k-th measurement of the j-th specimen under the i-th stress level, t is the time, ε_{ijk} is the random measurement error, K_i is the degradation rate under the i-th stress level, and b_i is the intercept under the i-th stress level.

3.2. The description of the universal method for lifetime prediction of MEMS gyroscope

On the basis of the above model assumptions, a universal method for lifetime prediction of MEMS gyroscope is proposed, as shown in Figure 3. Firstly, a long-term test platform for MEMS gyroscope is constructed, and the ADT scheme is designed. The degradation characteristic (bias instability) of MEMS gyroscope is extracted based on the output voltage of the MEMS gyroscope and Allan variance. In order to characterize the degradation trend of MEMS gyroscope, we propose the following steps:

Step 1, Convert the output voltage of the MEMS gyroscope to angular rate in each day, and then calculate the root mean square value of the angular rate in each day based on equation (2). Step 2, The bias instability of MEMS gyroscope in every day can be calculated by the least squares method, i.e. equation (6). Step 3, The degradation trend of bias instability in D days can be obtained. Step 4, Fit the degradation trend of bias instability with linear function.

Then the degradation model of MEMS gyroscope can be established. Because the accelerated stress in ADTs is temperature, so we use Arrhenius model as the acceleration model [17, 27, 35], and the degradation rate of the MEMS gyroscope can be expressed by:

$$\frac{dB_s(t)}{dt} = K = A\exp(-E / k_b T) \tag{28}$$

where k_B is the Boltzmann constant, which is 8.6171×10^{-5} eV/°C. T is the Kelvin temperature with a unit of K, A is an unknown parameter and E is the activation energy.

Taking the natural logarithm on both sides of equation (28) results in:

$$\ln\left(\frac{dB_s(t)}{dt}\right) = \ln A - E / k_b T \tag{29}$$

So, the activation energy E can be expressed as:

$$E = -k_b \frac{\partial\left[\ln\left(\dfrac{dB_s(t)}{dt}\right)\right]}{\partial\left(\dfrac{1}{T}\right)} \tag{30}$$

Integrating on the both two sides of equation (28) results in:

$$\int_0^{B_s^{cir}} d(B_s) = A\exp(-E / k_b T)\int_o^{TF} dt \tag{31}$$

where TF is the failure time and B_s^{cir} is failure threshold of bias instability.

So the failure time TF can be expressed as:

$$TF = \frac{B_s^{cir}}{A\exp(-E / k_b T)} \tag{32}$$

The acceleration factor model of MEMS gyroscope can be expressed as:

$$AF = \frac{TF_0}{TF_1} = \frac{\exp(-E / k_b T_1)}{\exp(-E / k_b T_0)} = \exp\left(\frac{E}{k_b}\left(\frac{1}{T_0} - \frac{1}{T_1}\right)\right) \qquad (33)$$

where TF_0 and TF_1 are failure time under normal stress and accelerated stress, T_0 and T_1 are normal temperature level and high temperature level.

As shown in equation (33), the acceleration factor model of MEMS gyroscope contains two unknown parameters, which can be estimated by least square method. Finally, the lifetime under normal stress level can be calculated by acceleration factor model and failure data under high stress level.
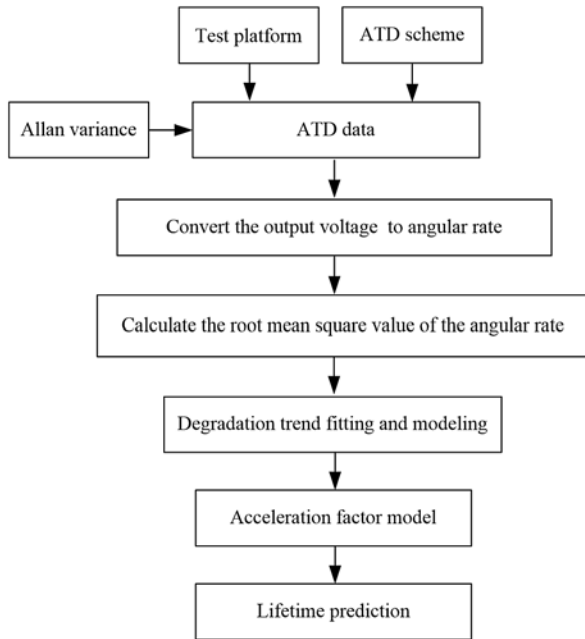

Fig. 3. The method diagram of lifetime prediction for MEMS gyroscope

4. Application Case

4.1. Design of ATD scheme and construction of test platform

According to GJB150.1-86, two accelerated stress levels were selected as S_1=45℃, S_2=60℃, and the normal temperature stress S_0=25℃. The number of specimens under each stress level was 4. Twelve MEMS gyroscopes, numbered 1#, 2#, 3#,..., 11#, 12#, were selected from the same batch MEMS gyroscopes. 1-4# MEMS gyroscopes were tested at 25℃ for 23 days, 5-8# MEMS gyroscopes were tested at 45℃ for 23 days, and 9-12# MEMS gyroscopes were tested at 60℃ for 23 days.

The test platform consists of E3631A power supply, NI PXLe-1071 data acquisition card, computer, constant temperature and humidity test chamber and multiple data lines, as shown in Figure 4. The E3631A power supply provides 5V voltage for the MEMS gyroscopes. The NI PXLe-1071 acquisition card can collect the output voltage of four MEMS gyroscopes simultaneously. It should be noted that Figure 4
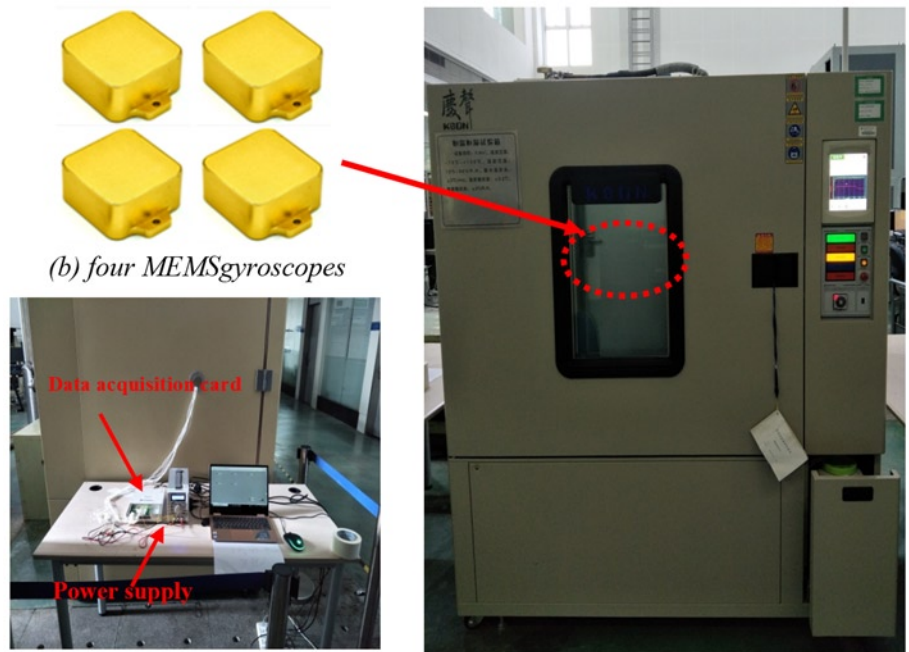
only lists the test environment at normal stress level. The remaining two accelerated stress tests also used the test platform shown in Figure 4, only changing the temperature of the constant temperature and humidity test chamber.

4.2. Analysis of test data

The output voltage of 12 MEMS gyroscopes at three constant stress levels are shown in Figure 5 (a) (b) (c). Allan variance curves at different stress level are shown in Figure 5 (d), all MEMS gyroscopes have line with slopes of −1/2 and 0 at lower correlation time, and have line with slope of 1/2 at different correlation time after the line with slope of 0. It indicates that the angular random walk, bias instability and rate random walk are the main characteristics in the output of MEMS gyroscopes.

In addition, as shown in Figure 5(d), no line with slope of −1 and +1 appear in the Allan variance curve, which indicates that the quantization noise and rate slope are not the main characteristics in the output of MEMS gyroscope. This is because the MEMS gyroscopes have no digital-to-analog conversion process from the output of capacitance to output of voltage, other scholars have same conclusions [12, 21, 26].

4.3. Degradation model

The degradation model of MEMS gyroscope can be established based on the test data and the new method. Step 1. Convert the output voltage of the 12 MEMS gyroscopes to angular rate, and then calculate the root mean square value of the angular rate every day based on the equation (2). Step 2. The bias instability of MEMS gyroscope in every day can be calculated by the least squares method, i.e. equation (6). Step 3. The degradation trend of bias instability in 23 days can be obtained. Step 4. Fit the degradation trend of bias instability with linear function. As shown in Figure 6, bias instability of all MEMS gyroscope increase approximately linearly with time at different temperature stress level. The degradation rates of each gyroscope under different temperature stress levels are shown in Table 1.

So the degradation model of the MEMS gyroscope based on Figure 6 and Table 1 can be expressed as:

(b) four MEMSgyroscopes

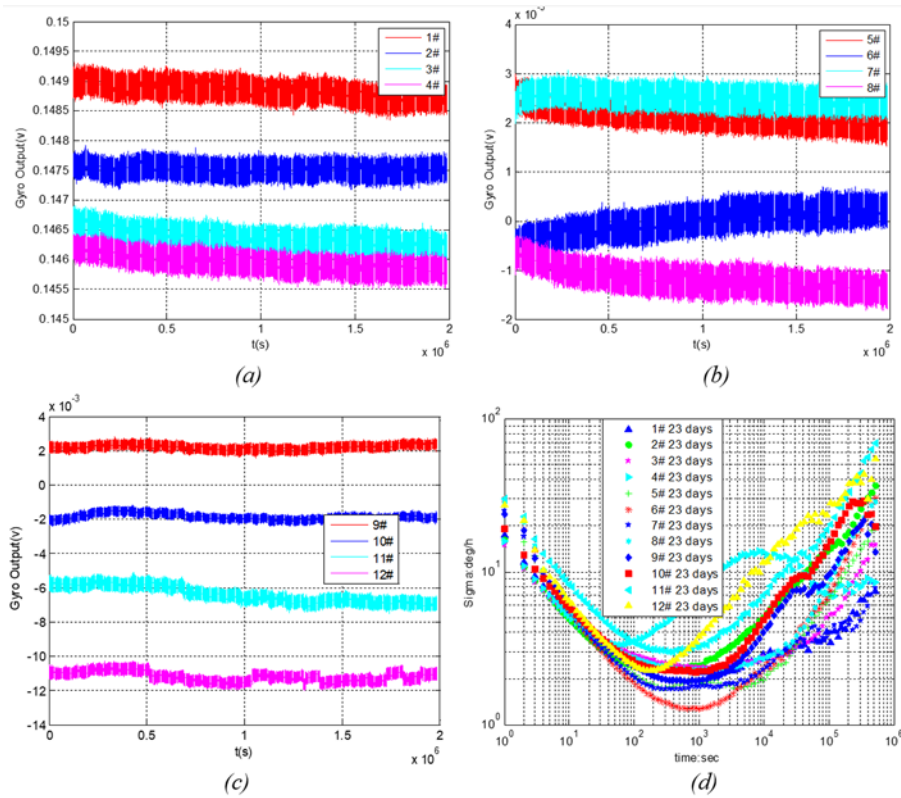*Fig. 4. Test platform of MEMS gyroscope under constant temperature stress*

Fig. 5. Voltage output and Allan variance curves of 12 MEMS gyroscopes under different temperature stresses

Table 1. Degradation rate of MEMS gyroscopes' bias instability at different temperature stress levels

Stress level		1#-12#MEMS				Mean
S_0	interception	4.2401	4.2174	4.4450	4.5752	4.3694
	degradation rate	0.0066	0.0132	0.0424	0.0178	0.0200
S_1	interception	1.6059	1.4122	0.8630	1.4004	1.3204
	degradation rate	0.0521	0.0137	0.0222	0.0316	0.0299
S_2	interception	1.5055	2.1970	1.4755	3.2460	2.1060
	degradation rate	0.0406	0.0241	0.0840	0.0507	0.0499

$$B_s(t) = Kt + b \qquad (34)$$

where b is the interception of the fitting line.

In addition, Table 1 shows that the degradation rate of bias instability is larger in higher temperature stress. This is consistent with the theoretical analysis results in Section 2.3. The degradation model of the MEMS gyroscope under different stress levels can be established by the mean values of degradation rate and intercept, which can be expressed as respectively:

$$B_s(t) = 0.0200t + 4.3694 \qquad (35)$$

$$B_s(t) = 0.0299t + 1.3204 \qquad (36)$$

$$B_s(t) = 0.0499t + 2.1060 \qquad (37)$$

4.4. Lifetime prediction

The literature shows that the failure threshold B_s^{cir} of the MEMS gyroscope is 25°/h [1-3]. The lifetime of 12 MEMS gyroscopes can be calculated based on equation (34) and Table 1, as shown in Table 2.

So the interception and degradation of the Arrhenius equation can be expressed as:

Table 2. The lifetime of 1#-12# MEMS gyroscope

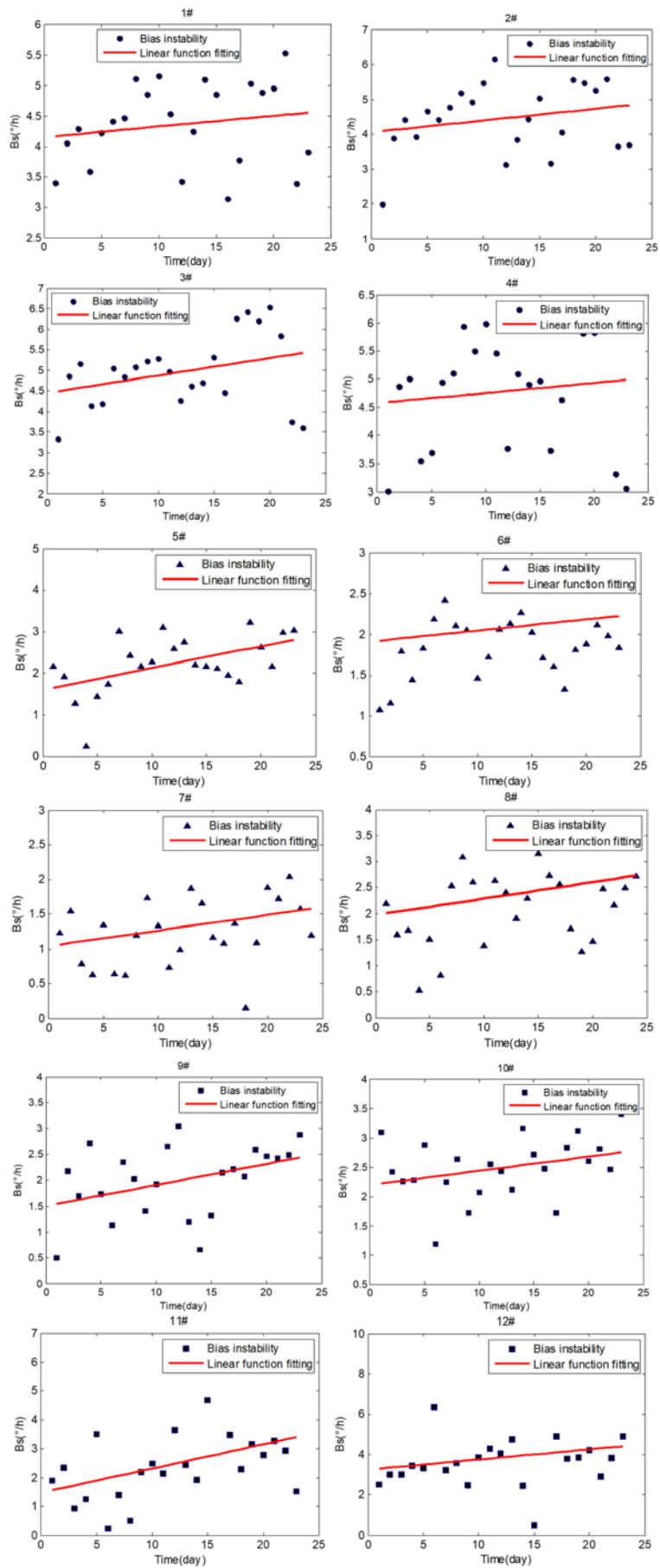| S_0	MEMS gyroscope	1#	2#	3#	4#	Mean
	lifetime	3145.4	1574.4	484.8	1147.5	1588.0
S_1	MEMS gyroscope	5#	6#	7#	8#	Mean
	lifetime	449	1721.7	1087.3	746.8	1001.2
S_2	MEMS gyroscope	9#	10#	11#	12#	Mean
	lifetime	578.7	946.2	280.1	429.1	558.5

Fig. 6. Bias instability of 12 MEMS gyroscopes changes with time under different temperature stresses

$$\ln A = 4.7868$$
$$\frac{E}{k} = 2592.2 \tag{38}$$

The parameter A and the activation energy E can be expressed as:

$$A = 119.9148$$
$$E = 0.2234 \tag{39}$$

So the acceleration factor model between the stress level S_0 and S_2 can be expressed as:

$$AF_{02} = \frac{TF_0}{TF_2} = \frac{\exp(-E/kT_2)}{\exp(-E/kT_0)} = \exp\left(\frac{E}{k}\left(\frac{1}{T_0} - \frac{1}{T_2}\right)\right)$$
$$= \exp\left(\frac{0.2234}{8.6171\times10^{-5}}\times\left(\frac{1}{25+273} - \frac{1}{60+273}\right)\right) = 2.4950 \tag{40}$$

The lifetime of MEMS gyroscope under normal stress level can be calculated based on the mean lifetime at stress level S_2 and equation (40):

$$TF_{S_0} = TF_{S_2}\bullet AF_{02} = 558.5\times2.4950 = 1393.5 \tag{41}$$

The lifetime calculated by acceleration factor model is close to the mean pseudo lifetime (1588 days) under different stress levels, the relative error is 12.25%.

Similarly, Substituting the mean degradation rate of MEMS gyroscope under stress level S_0 and S_1 into equation (34), the Arrhenius equation can be expressed as:

$$\ln(0.0200) = \ln A - \frac{E}{k}\frac{1}{25+273}$$
$$\ln(0.0299) = \ln A - \frac{E}{k}\frac{1}{45+273} \tag{42}$$

So the interception and degradation of the Arrhenius equation can be expressed as:

$$\ln A = 2.4818$$
$$\frac{E}{k} = 1905.4 \tag{43}$$

The parameter A and the activation energy E can be expressed as:

$$A = 11.9626$$
$$E = 0.1642 \tag{44}$$

So the acceleration factor model between the stress level S_0 and S_1 can be expressed as:

$$AF_{01} = \frac{TF_0}{TF_1} = \frac{\exp(-E/kT_1)}{\exp(-E/kT_0)} = \exp\left(\frac{E}{k}\left(\frac{1}{T_0} - \frac{1}{T_1}\right)\right)$$
$$= \exp\left(\frac{0.1642}{8.6171\times10^{-5}}\times\left(\frac{1}{25+273} - \frac{1}{45+273}\right)\right) = 1.4950 \tag{45}$$

The lifetime of MEMS gyroscope under normal stress level can be calculated based on the mean lifetime at stress level S_1 and equation (40):

$$TF_{S_0} = TF_{S_1}\bullet AF = 1001.2\times1.4950 = 1496.8 \tag{46}$$

The lifetime calculated by acceleration factor model is close to the mean pseudo lifetime (1588 days) under different stress levels, the relative error is 5.74%.

5. Conclusions

This paper establishes the degradation model and acceleration factor model of MEMS gyroscope based on Allan variance and ADTs, and proposes a universal lifetime prediction method for MEMS gyroscope. The main conclusions are as follows:

The degradation characteristic (bias instability) of MEMS gyroscope is extracted based on Allan variance, and the effect of temperature stress on the degradation rate of bias instability is analyzed. The theoretical analysis shows that the degradation rate of bias instability would increase with the increase of the temperature.

ADTs of MEMS gyroscope are designed and conducted, the experimental results indicate that bias instability of MEMS gyroscope increase approximately linearly with time at different temperature stress level, and the degradation rate of bias instability is larger in higher temperature stress.

Based on the theoretical analysis and experimental results above, the acceleration factor model of MEMS gyroscope under temperature stress is established, and the lifetime of the MEMS gyroscope is predicted. The presented methodology for lifetime prediction of MEMS gyroscope could reduce the testing duration and expense prominently. It may also be used as a reference for lifetime prediction for other MEMS devices.

References

1. Analog devices, ADXRS300 Data sheet, 2004. http://www.analog.com/static/imported -files/data_sheets/ADXRS300.pdf.
2. Analog devices, ADXRS646 Data sheet, 2011. https://www.analog.com/cn/products /adxrs 450.html.
3. Analog devices, ADXRS646 Data sheet, 2012. https://www.analog.com/cn/products/ adxrs646.html#product-overview.
4. Chateauneuf, and Alaa. Accelerated life testing and degradation modeling. Reliability Engineering System Safety 2014; 131: 228, https://doi.org/10.1016/j.ress.2014.05.004.
5. Chen Wenhua, Liu Juan, Gao Liang, et al. Accelerated degradation reliability modeling and test data statistical analysis of aerospace electrical connector. Chinese Journal of Mechanical Engineering 2011; 24(6): 957-962, https://doi.10.3901/ CJME2011.06.957.
6. Chien-Yu Peng and Sheng-Tsaing Tseng. Progressive-stress accelerated degradation test for highly-reliable products. IEEE Transactions on Reliability 2010; 59(1):30-37, https://doi. 10.1109/TR.2010.2040769.

7. Chikovani V V, Kyiv, Ukraine. Performance parameters comparison of ring laser, coriolis vibratory and fiber-optic gyros based on Allan variance analysis. IEEE 2nd International Conference Actual Problems of Unmanned Air Vehicles Developments. Proceedings 2013; 153-156, https://doi.org/10.1109/APUAVD.2013.6705312.

8. Chun-Lin Lu, Meng-Kao Yeh. Thermal stress analysis for a CMOS-MEMS microphone with various metallization and materials. Microelectronic Engineering 2019; 213: 47–54, https://doi.org/10.1016/j.mee.2019.04.013.

9. El-Sheimy N, Hou H, Niu X, et al. Analysis and modeling of inertial sensors using allan variance. IEEE Transactions on instrumentation and measurement 2007; 57(1): 140-149, https://doi.org/10.1109/tim.2007.908635.

10. Fu-Kwun Wang, Tao-Peng Chu. Lifetime predictions of LED-based light bars by accelerated degradation test. Microelectronics Reliability 2012; 52(7):1332–1336, https://doi. 10.1016/j.microrel.2012.02.019.

11. Grantham B E, Bailey M A. A least-squares normalized error regression algorithm with application to the Allan variance noise analysis method, In: Proceedings of IEEE/ION PLANS 2006; 750-755, https://doi.org/10.1109/PLANS.2006.1650671.

12. Heera Mallik M, Divya Jyothi K, Mithun S Varma, Divya Rao A. Agrawal. Minimum Variance Optimal Filter Design for a 3x3 MEMS Gyroscope Cluster Configuration. IFAC 2016; 49.1: 639-645, https://doi.org/10.1016/j.ifacol.2016.03.128.

13. Jacopo Iannacci. Reliability of MEMS: A perspective on failure mechanisms, improvement solutions and best practices at development level. Displays 2015; 37: 62-71, https://doi.org/10.1016/j.displa.2014.08.003.

14. Jianbin Su, Dingbang Xiao, Xiong Wang, Zhihua Chen, Xuezhong Wu. Vibration sensitivity analysis of the 'Butterfly-gyro' structure. Microsystem Technologies 2014; 20: 1281-1290, https://doi.org/10.1007/s00542-013-1913-x.

15. Jin-Won Joo and Sung-Hoon Choa. Deformation behavior of MEMS gyroscope sensor package subjected to temperature change. IEEE Transactions on Components and Packaging Technologies 2007; 30.2: 346-354, https://doi.org/10.1109/TCAP T.2007.897948.

16. Kim D, Thomas R, and Closkey M. Spectral analysis of vibratory gyro noise. IEEE tranc. Sensors 2013; 13(11): 4361-4374, https://doi.org/10.1109/JSEN.2013.2269797.

17. Kunsong Lin, Yunxia Chen, Dan Xu. Reliability assessment model considering heterogeneous population in a multiple stresses accelerated test. Reliability Engineering System Safety 2017; 165: 134-143, https://doi.org/10.1016/j. ress.2017.03.013.

18. Lawrence C N, Darryll J P. Characterization of ring laser gyro performance using the Allan variance method. Journal of Guidance, Control, and Dynamics 1997; 20 (1): 211-214, https://doi.org/10.2514/2.4026.

19. Liang Xue, Cheng-Yu Jiang, Hong-Long Chang, Yong Yang, Wei Qin, Wei-Zheng Yuan. A novel Kalman filter for combining outputs of MEMS gyroscope array. Measurement 2012; 45: 745-754, https://doi.org/10.1016/j.measurement.2011.12.016.

20. Lu X, Chen X, Wang Y, Tan Y. Consistency analysis of degradation mechanism in step-stress accelerated degradation testing. Eksploatacja i Niezawodnosc – Maintenance and Reliability 2017; 19 (2): 302-309, http://dx.doi.org/10.17531 /ein.2017.2.19.

21. Miroslav Matejček, Mikuláš Šostronek. New Experience with Allan Variance Noise analysis of accelerometers. October 2017; https://doi.org/10.23919/KIT.2017.8109457.

22. Mulloni V, Lorenzelli L, Margesin B, Barbato M, Meneghesso G. Temperature as an accelerating factor for lifetime estimation of RF-MEMS switches. Microelectronic Engineering, 2016; 160: 63-67, https://doi.org/ 10.1016/j.mee.2016.03.023.

23. Nelson W, Accelerated testing: statistical models, test plans, and data analysis. John Wiley & Sons: New York, 1990; NY. 10.1002/9780470316795.

24. Ningfang S, Yuan R, Jin J. Autonomous estimation of Allan variance coefficients of onboard fiber optic gyro. Journal of Instrumentation 2011; 6.09: P09005-P09005, https://doi.org/10.1088/1748-0221/6/09/P09005.

25. Oliveira V R B, Colosimo E A. Comparison of methods to estimate the time-to-failure distribution in degradation tests. Quality Reliability Engineering International 2004; 20(4): 363-73, https://doi.org/10.1002/qre.567.

26. Pin Lv, Jianye Liu, Jizhou Lai, Kai Huang. Allan variance method for gyro noise analysis using weighted least square algorithm. Optik 2015; 126: 2529-2534, https://doi.org/10.1016/j.ijleo.2015.06.044.

27. ReliaSoft Co. Accelerated Life Testing Reference. Tucson, AZ: ReliaSoft Publishing, 2014, https://www.ReliaSoft.com.

28. Richard J V, Ahmed S K. Statistical modeling of rate gyros. IEEE Transactions on Instrumentation and Measurement 2012; 61: 673-684, https://doi.org/10.1109/tim.2011.2171609.

29. Saeedivahdat A, Abdolkarimzadeh F, Feyzi A, Rezazadeh G, Tarverdilo S. Effect of thermal stresses on stability and frequency response of a capacitive microphone. Microelectronics Journal 2010; 41: 865-873.

30. Si X S, Wang W B, Hu C H, Zhou D H, Pecht M G. Remaining useful life estimation based on a nonlinear diffusion degradation process. IEEE Transactions on Reliability 2012; 61(1): 50-67, https://doi.org/10.1109/tr.2011.2182221.

31. Songhua Hao, Jun Yang, Christophe Berenguer. Nonlinear step-stress accelerated degradation modeling considering three sources of variability. Reliability Engineering System Safety 2018; 172: 207-215, https://doi.org/10.1016/j.ress.2017.12.012.

32. Tabata O, Tsuchiya T. Reliability of MEMS: testing of materials and devices. Weinheim, Wiley, 2006, https://doi.org/10.1007/s10800-008-9482-x.

33. Wang YS, Fang X, Zhang CH, Chen X, Lu JZ. Lifetime prediction of self-lubricating spherical plain bearings based on physics-of-failure model and accelerated degradation test. Eksploatacja i Niezawodnosc - Maintenance and Reliability 2016; 18(4): 528-538, https://doi.org/10.17531/ein.2016.4.7.

34. Wang Y, Zhang C, Chen X, Tan Y. Lifetime prediction method for electron multiplier based on accelerated degradation test. Eksploatacja i Niezawodnosc – Maintenance and Reliability 2014; 16 (3): 484-490.

35. Yang Z, Chen Y X, Li X F, Zio E, and Kang R. Smart electricity meter reliability prediction based on accelerated degradation testing and modeling. Electrical Power and Energy Systems 2014; 56: 209-219, https://doi.org/10.1016/j.ijepes.2013.11.023.

36. Zhiqiang X and Gebre-Egziabher D. Modeling and bounding low inertial sensor errors. In proc. IEEE/ION Position, Location and Navigation Symposium 2008: 1122-1132, https://doi.org/10.1109/PLANS.2008.4569999.

Yao LIU
Yashun WANG
Zhengwei FAN
Laboratory of Science and Technology on Integrated Logistics Support
College of Intelligence Science and Technology
National University of Defense Technology
Yanwachi str., Changsha, 410073, Hunan, China

Zhanqiang HOU
College of Intelligence Science and Technology
National University of Defense Technology
Yanwachi str., Changsha, 410073, Hunan, China

Shufeng ZHANG
Xun CHEN
Laboratory of Science and Technology on Integrated Logistics Support
College of Intelligence Science and Technology
National University of Defense Technology
Yanwachi str., Changsha, 410073, Hunan, China

E-mails: yaoliu133@126.com, wangyashun@nudt.edu.cn,
fanzhengwei15@nudt.edu.cn, houzhanqiang@nudt.edu.cn,
sfzhang@nudt.edu.cn, chenxun@nudt.edu.cnj237